34th Annual International Conference of the IEEE EMBS
San Diego, California USA, 28 August - 1 September, 2012

A Mesh-Based Approach for the 3D Analysis of Anatomical Structures of Interest in Radiotherapy

Aldo R. Mejia-Rodriguez , Elisa Scalco, Daniele Tresoldi, Anna M. Bianchi, Edgar R. Arce-Santana, Martin O. Mendez, Giovanna Rizzo

Abstract— **In this paper a method based on mesh surfaces approximations for the 3D analysis of anatomical structures in Radiotherapy (RT) is presented. Parotid glands meshes constructed from Megavoltage CT (MVCT) images were studied in terms of volume, distance between center of mass (distCOM) of the right and left parotids, dice similarity coefficient (DICE), maximum distance between meshes (DMax) and the average symmetric distance (ASD). A comparison with the standard binary images approach was performed. While absence of significant differences in terms of volume, DistCOM and DICE indices suggests that both approaches are comparable, the fact that the ASD showed significant difference (p=0.002) and the DMax was almost significant (p=0.053) suggests that the mesh approach should be adopted to provide accurate comparison between 3D anatomical structures of interest in RT.**

I. Introduction

THE analysis of anatomical structures of interest is a relevant task in the medical field. For example in Radiotherapy (RT), patients undergoing a head-and-neck cancer (HNC) treatment are known to experience significant decrease in the volume of the parotid glands and their migration toward the midline of the patient with a distance change of a few millimeters. Due to these anatomical modifications the parotids can receive a total dose significantly higher than the planned one. In this context the importance of the analysis of the anatomical modifications occurring during RT treatments is to both identify potential predictors of toxicity and design optimized adaptive treatment plans [1].

*A. R. Mejia-Rodriguez is with Institute of Molecular Bioimaging and Physiology (IBFM)-CNR, Milan, Italy and Bioengineering Department, Politecnico di Milano, Milan, Italy. Author is supported by CONACyT studentship (CVU/Becario): 217232/213579 for PhD studies (e-mail: armero83@gmail.com)

E. Scalco is with Institute of Molecular Bioimaging and Physiology (IBFM)-CNR, Milan, Italy

D. Tresoldi is with Institute of Molecular Bioimaging and Physiology (IBFM)-CNR, Milan, Italy and Bioengineering Department, Politecnico di Milano, Milan, Italy.

A.M. Bianchi is with Bioengineering Department Politecnico di Milano, Milan, Italy.

E. R. Roman-Arce is with Fac. de Ciencias, UASLP, San Luis Potosi, Mexico.

M.O. Mendez-Garcia is with Fac. de Ciencias, UASLP, San Luis Potosi, Mexico.

G. Rizzo is with Institute of Molecular Bioimaging and Physiology (IBFM)-CNR, Milan, Italy.

To have a better perspective of the distortions that occur in structures of interest, different techniques to represent structures in 3D have been implemented [2, 3]. The mesh data-structure is one of the most used techniques for rendering 3D objects and it is defined as a collection of vertices (points positioned in a virtual space), edges (a connection between two vertices) and faces (a closed set of edges) that defines the shape of a polyhedral object. The faces could form polygons of any type (quadrilaterals, concaves or convexes complex polygons) but triangular polygons are commonly used since this simplifies rendering [3].

Although meshing is widely used for rendering 3D geometrics, in RT, analysis of anatomical structures of interest is usually carried out by extracting quantitative measurements from a set of 2D binary images whose contours define a 3D surface [4, 5]. In this way a coarser representation of the structure surfaces is obtained [2].

In this paper, we propose a mesh-based approach to improve the analysis of 3D anatomical structures in RT. This approach is compared with the standard binary image approach in order to evaluate if the introduction of this more accurate 3D structure representation results in differences in structure analysis.

II. Methods

A. Analysis of structures of interest by meshes

Analysis of the 3D anatomical structures by meshes proposed in this paper consists in the calculation of nine quantitative standard indices. The indices could be divided into two categories, 1) indices that give spatial and geometrical information of an individual mesh: coordinates of the baricenter, surface area and volume; and 2) indices that make a comparison between two meshes: Euclidean distance between baricenters, surface area difference, volume difference, dice similarity coefficient (DICE) [1], maximum distance between meshes (DMax) and average symmetric distance (ASD) [1].

DICE index is a metric of the overlap between 2 surfaces ranging from 0 (no spatial overlap) to 1 (complete overlap). DMax index calculates the maximum distance between two surfaces and gives an idea of the worst local distance mismatch. ASD index is defined as the average Euclidean distance between two surfaces, which is 0 for a perfect match.

For the calculations of the meshes and the set of indices the standard libraries included in the Visualization Toolkit (VTK) package were used, particularly the VTK package implemented for its use in Python [6].

B. Boolean operations on meshes

For DICE, DMax and ASD calculations, a set of classes that enable computation of boolean operations on meshes were used [7]. Boolean operations over meshes can be computed using the signed distance field (distance from a point x in one mesh to the nearest point on the surface defined by another mesh). The sign of the distance field corresponds to whether a point is inside (negative), outside (positive), or on (zero) the other mesh. In this context, the boolean operations of union, intersection and difference were defined as:

- Union: set of cells in each mesh such that the distance from each cell point to the other mesh is ≥ 0.
- Intersection: set of cells in each mesh such that the distance from each cell point to the other mesh is ≤ 0.
- Difference: set of cells of the mesh A (M_A) whose points are a non-negative distance from mesh B (M_B) combined with the cells of M_B whose points are a non positive distance from M_A.

Taking these assumptions into account and given two meshes A and B, the DICE, ASD and DMax indices were calculated as:

$$DICE = 2\frac{V_A \bigcap V_B}{V_A + V_B} \quad (1)$$

$$ASD = \frac{1}{M_A + M_B}\left(\sum_{p_B \in M_A} d(p_A, M_B) + \sum_{p_A \in M_B} d(p_B, M_A) \right) \quad (2)$$

$$DMax = \max\left\{ \max_{p_A \in M_A} d(p_A, M_B), \max_{p_B \in M_B} d(p_B, M_A) \right\} \quad (3)$$

where V_A and V_B are the sets of cells within A and B, respectively, $d(p_A, M_B)$ and $d(p_B, M_A)$ indicate the shortest distance between an arbitrary point to A or B, respectively.

The same equations can also be used to define correspondent indices for the standard binary image analysis, where, instead of meshes, A and B refer to binary image contours.

Fig. 1 shows an example of two meshes to be compared and the respective meshes generated by the boolean operations.

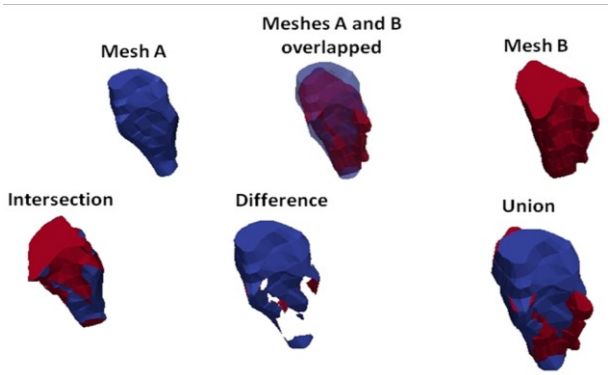

Fig. 1 Example of 3D representation of two meshes: A and B, with their respective boolean operations meshes.

C. Comparison between mesh and binary image approaches for the analysis of 3D structures

Mesh analysis was applied to a set of Megavoltage CT (MVCT) images from 10 patients treated for HNC with Helical Tomotheraphy analyzed in [1] with the standard analysis based on binary images. Triangular mesh surfaces corresponding to the right and left parotids were constructed from the manual contour delineation by three different expert observers in radiological images using the power crust method [8]; the set of binary images used for the parotid analysis studied in [1] were also generated using these manual contour delineations.

A comparison between measurements calculated from binary images in [1] and measurements computed from meshes was made in terms of parotid volumes, distance between right and left parotids center of mass (DistCOM), DICE, ASD and DMax indices. Wilcoxon signed rank test ($p<0.05$) between both approaches was used to assess the comparison.

III. Results

Table I presents the results for the calculation of the volume of the parotid glands from both meshes and binary images. For each patient mean ± std values of the right parotid (*Par R*) and left parotid (*Par L*) are presented. The comparison between mesh and binary images volume values was assessed for each expert observer (Exp). The mean ±std values found for Exp1 were 16.759±5.132 cm^3 vs. 16.760±5.129 cm^3; Exp2 16.377±5.023 cm^3 vs. 16.405±5.037 cm^3; and Exp3 18.304±5.107 cm^3 vs. 18.166±5.044 cm^3, for mesh approach and binary image approach respectively. No significant differences were found (Exp1 p =0.668; Exp2 p=0.861 ; Exp3 p=0.538).

Table II shows the comparison for DistCOM of the right and left parotids. The mean ± std values found for Exp1 were 110.55±8.64 mm vs. 111.44±8.44 mm; Exp2 109.97±8.52 mm vs. 111.03±8.55 mm; and Exp3 109.55±7.88mm vs. 110.40±7.68 mm. No significant differences were found (Exp1 p = 0.623; Exp2 p=0.677 ; Exp3 p=0.677).

Table III presents the results for DICE, DMax and ASD indices; for each patient the mean ± std value of all possible

pairs comparisons between the three expert observers are presented. The mean ± std values of the mesh and binary images estimations respectively for each index were: DICE 0.796±0.043 vs. 0.812±0.028; DMax 9.014±2.052 mm vs. 9.617±1.840 mm; and ASD 1.157±0.429 mm vs. 1.581±0.250 mm. No significant differences were found for the DICE (p=0.179) and DMax (p=0.053), while ASD shows significant differences (p=0.002) between mesh and binary image approaches.

IV. Discussion

Volume and DistCOM give geometrical and spatial information of a structure of interest, in this case parotid glands from patients treated with RT. The absence of significant differences between the mesh-based analysis and the approach based on sets of binary images suggests that both methodologies are suitable to provide quantitative anatomical information in parotid glands. DICE, DMax and ASD allow comparisons between two structures; in this case allowed to compare the parotid glands 3D representations constructed from the manual contours delineated by three different expert observers in RT. Results showed that the two approaches studied in this work are comparable in terms of DICE and DMax, but showed significant difference (21%) when ASD is considered.

Volume, DistCOM and DICE indices give spatial global information about the structures analyzed, therefore these indices are less susceptible to the variations presented in the mesh-based rendering and the representation using binary images; hence, the absence of significance between the two approaches was expected. On the other hand, ASD and DMax indices are more sensitive to these variations because they give information about the mean mismatch and the worst mismatch case between 2 structures respectively. The fact that the ASD showed significant difference (p=0.002) and the DMax was almost significant (p=0.053) suggests that mesh-based analysis presented in this paper should be preferable to obtain geometrical information of 3D structures. Besides, an additional advantage related to the use of a mesh approach is that it facilitates modeling of complex deformations, such as the ones that could be found in RT.

V. Conclusion

The mesh approach presented in this work could represent a useful tool in RT to compare anatomical structures of interest, being able to provide a finer 3D shape representation. This approach could have more relevance when anatomical structures with more complex or deformable shapes, like the lungs, are considered.

TABLE I. VOLUME COMPARISON BETWEEN MESH AND BINARY IMAGES APPROACHES. VALUES WERE CALCULATED FOR RIGHT (R) AND LEFT (L) PAROTIDS FOR EACH PATIENT (PAT)

VOLUME (cm^3)

	Exp1		Exp2		Exp3	
	Mesh	**Binary**	**Mesh**	**Binary**	**Mesh**	**Binary**
Pat1 R	18.540	18.540	19.836	20.190	23.340	23.340
Pat1 L	21.500	21.500	20.650	20.650	22.434	22.430
Pat2 R	17.693	17.690	18.343	18.340	19.626	19.630
Pat2 L	19.131	19.130	16.799	17.020	20.674	18.500
Pat3 R	17.566	17.570	16.691	16.690	19.310	19.310
Pat3 L	10.225	10.260	15.005	15.000	13.630	13.630
Pat4 R	17.350	17.350	21.825	21.820	20.273	20.270
Pat4 L	17.282	17.280	18.019	18.020	17.023	17.020
Pat5 R	22.938	22.940	24.334	24.330	22.975	22.980
Pat5 L	21.703	21.700	17.327	17.330	22.832	22.830
Pat6 R	24.590	24.590	20.068	20.070	28.834	28.830
Pat6 L	26.204	26.200	21.145	21.140	19.952	19.950
Pat7 R	14.082	14.080	13.341	13.340	15.121	15.180
Pat7 L	17.724	17.720	15.875	15.880	17.878	17.880
Pat8 R	7.896	7.900	5.399	5.400	10.666	10.670
Pat8 L	10.393	10.390	9.104	9.050	11.167	11.170
Pat9 R	11.463	11.460	12.111	12.110	11.002	11.000
Pat9 L	10.738	10.740	7.164	7.210	10.658	10.660
Pat10 R	15.698	15.700	20.629	20.630	23.076	22.440
Pat10 L	12.460	12.460	13.880	13.880	15.601	15.600
MEAN	**16.759**	**16.760**	**16.377**	**16.405**	**18.304**	**18.166**
STD	**5.132**	**5.129**	**5.023**	**5.037**	**5.107**	**5.044**

No significant differences were found with the Wilcoxon signed rank test ($p<0.05$).

TABLE II. DISTCOM COMPARISON BETWEEN MESH AND BINARY IMAGES APPROACHES. VALUES WERE CALCULATED FOR RIGHT (R) AND LEFT (L) PAROTIDS FOR EACH PATIENT (PAT)

DistCOM_ (mm)

	Exp1		Exp2		Exp3	
	Mesh	**Binary**	**Mesh**	**Binary**	**Mesh**	**Binary**
Pat1	115.77	116.53	115.66	116.16	113.17	114.45
Pat2	106.06	107.20	106.68	107.53	106.19	107.10
Pat3	112.78	113.18	114.27	115.31	115.24	115.57
Pat4	113.11	113.39	109.49	109.57	110.42	109.29
Pat5	121.49	122.47	121.81	123.82	119.16	120.48
Pat6	122.22	122.83	119.23	120.76	117.42	118.37
Pat7	98.09	99.08	95.56	97.79	96.10	98.56
Pat8	99.09	100.19	99.45	100.35	98.31	99.52
Pat9	102.90	104.53	104.09	104.70	105.96	105.20
Pat10	113.98	114.97	113.41	114.35	113.54	115.42
MEAN	**110.55**	**111.44**	**109.97**	**111.03**	**109.55**	**110.40**
STD	**8.64**	**8.44**	**8.52**	**8.55**	**7.80**	**7.68**

No significant differences were found with the Wilcoxon signed rank test ($p<0.05$).

TABLE III.

DICE, DMAX AND ASD COMPARISONS BETWEEN MESH AND BINARY IMAGES APPROACHES. VALUES WERE CALCULATED FOR RIGHT (R) AND LEFT (L) PAROTIDS FOR EACH PATIENT (PAT).

	DICE				**DMax (mm)**				**ASD (mm)**			
	Mesh		**Binary Im.**		**Mesh**		**Binary Im.**		**Mesh**		**Binary Im.**	
	Mean	**std**	**Mean**	**Std**	**Mean**	**std**	**Mean**	**std**	**Mean**	**std**	**Mean**	**std**
Pat1 R	0.790	0.018	0.788	0.019	10.612	0.708	9.844	0.450	1.208	0.224	1.895	0.053
Pat1 L	0.822	0.009	0.809	0.025	9.618	0.751	13.834	2.672	1.102	0.082	1.832	0.209
Pat2 R	0.840	0.018	0.836	0.007	6.760	2.382	8.469	1.000	0.570	0.209	1.326	0.083
Pat2 L	0.785	0.019	0.828	0.031	10.280	1.630	9.199	1.455	0.960	0.342	1.457	0.296
Pat3 R	0.769	0.063	0.771	0.040	8.464	1.161	8.859	1.499	0.981	0.465	1.941	0.458
Pat3 L	0.786	0.028	0.808	0.064	7.699	1.404	8.113	2.114	1.393	0.461	1.490	0.481
Pat4 R	0.767	0.054	0.774	0.026	11.374	3.690	11.770	1.603	1.503	0.457	1.881	0.238
Pat4 L	0.809	0.033	0.793	0.020	8.792	0.252	10.324	1.138	0.901	0.212	1.589	0.129
Pat5 R	0.843	0.001	0.838	0.011	6.731	1.017	8.117	0.814	0.729	0.077	1.473	0.084
Pat5 L	0.788	0.028	0.812	0.017	8.194	1.276	10.301	1.927	0.940	0.323	1.646	0.110
Pat6 R	0.808	0.021	0.855	0.028	10.900	1.986	8.949	3.859	0.989	0.848	1.434	0.305
Pat6 L	0.841	0.441	0.827	0.029	7.992	1.882	9.013	0.825	1.695	0.930	1.613	0.315
Pat7 R	0.730	0.044	0.786	0.028	8.786	1.892	10.983	0.645	1.350	0.585	1.721	0.220
Pat7 L	0.825	0.034	0.813	0.032	7.789	0.825	8.103	0.849	0.886	0.264	1.567	0.266
Pat8 R	0.703	0.104	0.824	0.053	13.578	4.264	6.548	2.908	2.364	0.583	1.391	0.473
Pat8 L	0.837	0.037	0.825	0.027	7.053	1.162	8.231	3.042	1.001	0.299	1.226	0.176
Pat9 R	0.874	0.042	0.878	0.024	6.483	1.863	9.436	3.206	0.625	0.273	1.028	0.207
Pat9 L	0.748	0.069	0.817	0.044	7.359	0.947	8.024	2.011	1.192	0.442	1.422	0.321
Pat10 R	0.753	0.044	0.791	0.026	13.115	3.069	13.327	2.958	1.768	0.229	1.953	0.278
Pat10 L	0.803	0.019	0.771	0.011	8.707	0.448	10.893	0.722	0.979	0.201	1.743	0.126
MEAN	**0.796**		**0.812**		**9.014**		**9.617**		***1.157**		**1.581**	
STD	**0.043**		**0.028**		**2.052**		**1.840**		**0.429**		**0.250**	

* p=0.002, ASD presented significant difference with the Wilcoxon signed rank test

REFERENCES

[1] E. Faggiano, C. Fiorino, E. Scalco, S. Broggi, M. Cattaneo, E. Maggiulli, I. Dell'Oca, N. Di Muzio, R. Calandrino,G. Rizzo, "An automatic contour propagation method to follow parotid gland deformation during head-and-neck cancer tomotherapy", *Phys Med Biol.* 2011 Feb 7;56(3):775-91. Epub 2011 Jan 14.

[2] A. M. Alyassin, J. L. Lancaster, J. Hunter Downs III, and P. T. Fox, "Evaluation of new algorithms for the interactive measurement of surface area and volume", *Med. Phys. 21*, 741, 1994.

[3] C. Smith. " On Vertex-Vertex Systems and their Use in Geometric and Biological Modelling". Ph.D. Dissertation. University of Calgary, Calgary, Alta., Canada, 2006.

[4] R. Allozi, X.A. Li, J. White, A. Apte, A. Tai, J.M. Michalski, W.R. Bosch, I.E. Naqa, "Tools for consensus analysis of experts' contours for radiotherapy structure definitions", *Radiotherapy and Oncology*, Volume 97, Issue 3, December 2010, Pages 572-578.

[5] W.Y. Song, B. Chiu, G.S. Bauman, M. Lock, G. Rodrigues, R. Ash, C. Lewis, A. Fenster, J.J. Battista, J. Van Dyk, "Prostate contouring uncertainty in megavoltage computed tomography images acquired with a helical tomotherapy unit during image-guided radiation therapy", *Int J Radiat Oncol Biol Phys*. 2006 Jun 1;65(2):595-607.

[6] W. Schroeder, K. Martin, B. Lorensen 2002 *The Visualization Toolkit 2nd edn* (Upper Saddle River, NJ: Prentice-Hall).

[7] C. Quammen, C. Weigle, R. M. Taylor II, "Boolean Operations on Surfaces in VTK Without External Libraries" VTK Journal, May 2011.

[8] N. Amenta, S. Choi, R. K. Kolluri, "The power crust, unions of balls, and the medial axis transform", *Computational Geometry*, Volume 19, Issues 2–3, July 2001, Pages 127-153.

[9] E. Scalco, E. Faggiano, S. Liberini, C. Fiorino, E. Maggiulli, S. Broggi, G. M. Cattaneo, R. Calandrino, G. Rizzo, "Validation of elastic registration to study parotid deformation in head and neck Tomotherapy", *Radiotherapy & Oncology*, 2011. 99, Supplement 1, p S339.